The Astronomical Journal, 131:34–40, 2006 January

NEAR-INFRARED SEARCH FOR C IV ABSORPTION COUNTERPARTS ALONG THE LINES OF SIGHT TO PAIR QUASARS[1,2]

Toru Misawa,[3] Nobunari Kashikawa,[4,5] Youichi Ohyama,[6] Tetsuya Hashimoto,[7] and Masanori Iye[4,5,7]

Received 2005 June 15; accepted 2005 September 21

ABSTRACT

We carried out a Subaru and UKIRT near-infrared imaging survey for Hα-emitting galaxies around two pair quasar systems (Q0301−005/Q0302−003 and Q2343+125/Q2344+125) and a triple quasar system (KP 76/KP 77/KP 78). Narrowband near-infrared filters covering the Hα emission expected for galaxies at the confirmed C IV absorption redshift toward the quasar systems were used for this survey. These quasar pairs or triplet are separated at most by 17′ ($\sim$5 h^{-1} Mpc in proper distance) from each other on the sky and have common C IV absorption lines at almost identical redshifts at $z = 2.24$–2.43, which suggests there could be a megaparsec-scale absorbing system such as a cluster, or a group, of galaxies that covers all the lines of sight to the pair/triple quasars. Using narrowband deep images, we detected five candidates for Hα-emitting galaxies around two of the six fields, Q2343+125 and Q2344+125, whose apparent star formation rates are extremely high, 20–466 $M_\odot$ yr^{-1}. However, all or most of them are not likely to be galaxies at the absorption redshift but galaxies at lower redshift, because of their extreme brightness. In the fields of the other quasars, we detected no star-forming galaxies, nor did we find any number excess of galaxy counts around them. These nondetections could be because the luminosities and star formation rates of galaxies are lower than the detection limits of our observations ($K' > 21$ and SFR < 1.8–$240\,h^{-2}\,M_\odot$ yr^{-1}). They could be located outside of the observed field around Q0301 and Q0302, since our targeting field covers only 2% of this pair quasar field. But this is not the case for the other pair/triple quasar fields, because we found large field coverage fractions ($\sim$33%–75%). Otherwise, most C IV absorption lines could be ascribed not to clusters of galaxies but to isolated star-forming pockets, far from bright galaxies, that could be analogous objects to weak Mg II absorbers.

Key words: galaxies: evolution — quasars: absorption lines — quasars: individual (Q0301−005, Q0302−003, KP 76, KP 77, KP 78, Q2343+125, Q2344+125)

1. INTRODUCTION

Several quasars, which are separated from each other on the sky by a few arcminutes, sometimes have common metal-absorption lines at almost identical redshifts (e.g., Shaver et al. 1982; Jakobsen et al. 1986; Crotts & Fang 1998). The presence of such common metal-absorption lines implies that megaparsec-scale gas clouds exist at that redshift, and that they are covering both lines of sight to the quasars. Since it is difficult to assume that a single homogeneous megaparsec-scale absorber covers both the lines of sight to those quasar pairs based on the framework of the widely accepted cold dark matter (CDM)–dominant universe, these metal lines could be produced by gas clouds that are clustering and forming a megaparsec-scale system (e.g., clouds in galaxies that are members of a megaparsec-scale cluster [group] of galaxies). Francis & Hewett (1993) estimated the probability of having strong Lyα absorption lines (i.e., analog of metal lines) at almost the same redshift in two lines of sight separated by a few arcminutes is of order 10^{-4}. If there is a cluster (group) of galaxies, the probability would be increased. Although several high-z clusters of galaxies have been recently discovered, it is still observationally difficult to detect emission lines of star-forming galaxies in the redshift desert at $z > 1.5$. However, observations around pair quasars with common metal-absorption systems are quite promising (e.g., Francis et al. 1996). High-z clusters of galaxies are excellent targets for investigating star formation histories.

To date, several clusters (groups) of galaxies have been detected at $z > 2$. They are often detected around radio-loud quasars or radio galaxies. Pentricci et al. (2000) found 14 Lyα-emitting galaxies within the projected distance of 1.5 Mpc from the powerful radio galaxy Q1138−262 at $z = 2.16$. Pascarelle et al. (1996) also detected two Lyα-emitting galaxies at $z \sim 2.39$ in the field around the weak radio galaxy, 53W002, and also confirmed them spectroscopically. There are several other candidates for clusters (groups) of galaxies at $z > 2$ discovered by narrowband (NB) imaging observations (e.g., LeFèvre et al. 1996; Hu & McMahon 1996). Not only Lyα but also Hα and [O III] are also useful lines for identification of star-forming galaxies (e.g., Teplitz et al. 1998; Iwamuro et al. 2000). Galaxies have also been discovered in the fields around quasars as counterparts of strong absorption systems. C IV absorption systems with rest-frame equivalent width $W_{\rm rest} > 0.4$ Å and Mg II absorption systems with $W_{\rm rest} > 0.3$ Å are thought to have $\sim$70 and $\sim$40 kpc sizes around L^* galaxies, respectively, by comparing the Press-Schechter function (as luminosity function of galaxy) and the number densities of these absorption systems per redshift. Charlton & Churchill (1996) showed by performing a Monte Carlo simulation that both spherical halo and randomly oriented disks with only 70%–80% covering factors of gas clouds can recover the observed properties

[1] Based on data collected at Subaru Telescope, which is operated by the National Astronomical Observatory of Japan.
[2] Based on data collected at the United Kingdom Infrared Telescope (UKIRT), which is operated by the Joint Astronomy Centre on behalf of the UK Particle Physics and Astronomy Research Council.
[3] Department of Astronomy and Astrophysics, Pennsylvania State University, 525 Davey Laboratory, University Park, PA 16802; misawa@astro.psu.edu.
[4] National Astronomical Observatory, 2-21-1 Osawa, Mitaka, Tokyo 181-8588, Japan.
[5] Department of Astronomical Science, Graduate University for Advanced Studies, 2-21-1 Osawa, Mitaka, Tokyo 181-8588, Japan.
[6] Department of Infrared Astrophysics, Institute of Space and Astronautical Science, Japan Aerospace Exploration Agency, 3-1-1 Yoshinodai, Sagamihara, Kanagawa 229-8510, Japan.
[7] Department of Astronomy, School of Science, University of Tokyo, 7-3-1 Hongo, Bunkyo-ku, Tokyo 113-0033, Japan.

of Mg II absorbers. This means that the distribution of the Mg II absorbers around galaxies is not smooth but patchy. There are some galaxy surveys around *single* quasars (e.g., Bergeron & Boissé 1991; Steidel et al. 1994; Lanzetta et al. 1998; Chen et al. 2001a, 2001b). However, for *pair* quasar regions, only a few observations have been carried out based on common metal-absorption lines of pair quasars (e.g., Teplitz et al. 1998; Francis et al. 1997, 1996), in spite of the high potential for finding galaxies.

In this paper, we report the results of our near-infrared (NIR) NB imaging survey of the fields around pair/triple quasars that have common metal-absorption lines at $z \sim 2.3$. They are separated at most by $17'$ [$\sim 5\ h^{-1}$ Mpc in proper distance, with $h = H_0/(72\ \mathrm{km\ s^{-1}\ Mpc^{-1}})$]. Our objectives are to search for star-forming galaxies that produce the common metal-absorption lines and see if there are galaxies that are members of the cluster (or group) of galaxies that includes those star-forming galaxies.

We present the outline of the observations and data reduction in § 2 and the brief description of the photometric analysis in § 3. In § 4, we present the result for each quasar field. We summarize and discuss our results in § 5. Throughout this paper, we assume $H_0 = 72\ \mathrm{km\ s^{-1}\ Mpc^{-1}}$, $\Omega_0 = 0.3$, $\Omega_\Lambda = 0.7$, and $q_0 = 0.5$.

2. OBSERVATION AND DATA REDUCTION

We observed the fields of pair/triple quasars. These quasars have common absorption systems (that at least contain C IV doublets in them) with a small redshift difference, $\Delta z \sim 0.005$, which corresponds to a velocity difference, $\Delta v \sim 500\ \mathrm{km\ s^{-1}}$, in the frame of the absorbers. However, we should notice that if the redshift difference is caused by the Hubble flow, these absorbers would be separated by much larger than the typical size of a cluster of galaxies along the line of sight. We chose NB filters that cover redshifted Hα emission lines. The filter name, central wavelength, bandwidth, corresponding redshift for Hα emission line detection, and the bandpass ratio of NB to broad band (K' band) are listed in Table 1. To see the color excess, we also carried out K'-band imaging observations. The observations were performed with either the Cooled Infrared Spectrograph and Camera for OHS (CISCO; Motohara et al. 1998) on the Subaru Telescope (Iye et al. 2004) or the UKIRT First-Track Imager (UFTI; Roche et al. 2003) on the UKIRT. Both instruments have HAWAII 1024×1024 pixel HgCdTe arrays that cover a field of view (FOV) of $108'' \times 108''$ and $92'' \times 92''$, respectively. We summarize the observation logs in Table 2; columns (1) and (2) are the quasar name and its emission redshift, respectively. The absorption redshift of the common metal lines is given in column (3). The identified ion transition is listed in column (4). The data were taken on the date in column (6) using the filter in column (5). Exposure time and average seeing size are in columns (7) and (8), respectively. Columns (9) and (10) are detection limits with 3 and 5 σ levels, which are magnitudes of the faintest artificial objects that are placed in the observed frame and extracted with 3 or 5 σ detection levels, respectively. We describe the simulation in detail in § 3. In columns (11) and (12) we also present 3 σ detection limits for the Hα emission line and the corresponding star formation rate. References of spectroscopic observations are given in column (13).

Data reduction was done in a standard manner with IRAF. All objects are identified by the SExtractor program (Bertin & Arnouts 1996) with a detection threshold of 2.0 σ. We evaluated the magnitudes of objects in circular apertures twice as large as the seeing size.

TABLE 1
TRANSMISSION OF NB FILTERS

Filter (1)	λ_{cen}[a] (μm) (2)	$\Delta\lambda$[b] (μm) (3)	$z(\mathrm{H}\alpha)$[c] (4)	$\Delta\lambda_{\mathrm{NB}}/\Delta\lambda_{K'}$[d] (%) (5)
2.122[e]	2.119	0.031	2.229	9.1
2.248S[e]	2.253	0.035	2.433	10.3
$H_2(2-1)$[f]	2.250	0.022	2.428	6.9
$H_2(1-0)$[f]	2.120	0.020	2.230	6.3

[a] Central wavelength of the filter.
[b] Bandpass width of the filter with 50% transmission.
[c] Redshift of a star-forming galaxy whose Hα emission line is redshifted into the center of the filter.
[d] Bandpass ratio of NB to K'-band filters.
[e] Filter available with UKIRT + UFTI.
[f] Filter available with Subaru + CISCO.

3. PHOTOMETRIC ANALYSIS

In the color-magnitude (CM) analysis to isolate Hα-emitting objects, we need an accurate evaluation of the photometric errors. Therefore, we have created 10,000 artificial stars with the seeing size of each frame. Their magnitude distribution is homogeneous between $K' = 15$ and 22 mag. We placed them in both K' and NB frames randomly. We plot CM diagrams to compare the detected objects against the simulated artificial objects. The candidates for intervening galaxies at $z \sim 2.3$ have $K' - \mathrm{NB}$ color excesses because their Hα emission lines are redshifted into the NB filter bandpass, which makes them deviate from the distributions of the artificial objects. We regard all the objects as candidate Hα emitters, if they deviate toward the positive direction in the vertical axis (i.e., $K' - \mathrm{NB}$) by more than 3 σ from the distribution of the artificial objects in the CM diagrams. It is unlikely that the color excess is caused by other lines whose rest-frame wavelength are shorter than Hα, such as Lyα, [O II], or [O III], because the galaxies would be at $z \sim 17.5$, 5.0, and 3.5, respectively, if these lines are redshifted into the bandpass of the NB filters. The flux of these objects would be too weak to detect in our observations. On the other hand, if the candidate objects are much brighter than the typical magnitudes of Hα-emitting galaxies that produce metal absorption lines, $J \sim 22.5$, $H \sim 21.5$, and $K \sim 20.8$ (Teplitz et al. 1998), these color excesses could be due to NIR emission lines from galaxies at lower redshift, such as [Fe II] 1.257 μm, [Fe II] 1.644 μm, Paα, Paβ, and Brγ, which is described in § 5.

If we assume that the color excess is attributed to Hα emission lines, we can estimate the flux of the Hα line from the K' and NB magnitudes by

$$K' - \mathrm{NB} = 2.5 \log\left[1 \pm 10^{(K'-\gamma)/2.5}\right] + K'_0 - \mathrm{NB}_0, \quad (1)$$

where K'_0 and NB_0 are magnitude zero points (i.e., a magnitude corresponding to the flux of 1 count $\mathrm{s^{-1}}$ on each pixel) for K' and NB filters, respectively (e.g., Iwamuro et al. 2000). Here, the constant, γ, is defined as

$$\gamma = K'_0 - 2.5 \log\left(\frac{f_{\mathrm{H}\alpha}}{W_{\mathrm{NB}}}\right), \quad (2)$$

where W_{NB} is the bandwidth of the NB filter and $f_{\mathrm{H}\alpha}$ is the total Hα line flux (without the continuum flux) that is covered by the NB filters. We define 1, 2, and 3 σ deviation borders in the CM diagram from equation (1) with a fixed γ-value that covers 68.3%, 95.5%, and 99.7% of all the artificial objects, respectively.

TABLE 2

OBSERVATION LOG

QSO (1)	z_{em} (2)	z_{abs} (3)	Ion (4)	Filter (5)	Date (6)	Exposure (s) (7)	Seeing (arcsec) (8)	3 σ (mag) (9)	5 σ (mag) (10)	$f_{H\alpha}$(limit)[a] (ergs s^{-1} cm^{-2}) (11)	SFR(limit)[b] (h^{-2} $M_{\odot}$ yr^{-1}) (12)	Reference (13)
KP 76[c]	2.467	2.2462	C IV, Si IV	K98	2002 May 24–25	11760	0.42	21.39	21.03	2.4×10^{-17}	6.8	1
				2.122	2002 May 24–25	33100	0.42	20.91	20.39			
KP 77/KP 78[d]	2.526, 2.605	2.2445, 2.2417	C IV, Si IV	K'	2003 May 14	1440	0.40	21.09	20.42	6.3×10^{-18}	1.8	1
				$H_2(1-0)$	2003 May 14	5760	0.39	20.00	19.34			
Q0301−005[c]	3.223	2.4291	C IV, Si IV	K98	2002 Dec 22–23	4860	0.82	20.06	19.34	6.9×10^{-16}	236	2
				2.248S	2002 Dec 22–23	11700	0.88	18.77	18.14			
Q0302−003[c]	3.285	2.4233	C IV, Si IV	K98	2002 Dec 22	4860	0.48	21.07	20.44	6.7×10^{-17}	23	2
				2.248S	2002 Dec 22	12600	0.50	20.15	19.59			
Q2343+125[d]	2.515	2.4285, 2.4308	C IV	K'	2000 Nov 19	3260	0.94	20.54	20.03	1.6×10^{-17}	5.5	3
				$H_2(2-1)$	2000 Nov 19	8640	0.93	19.21	18.51			
Q2344+125[d]	2.763	2.4265, 2.4292	C IV	K'	2003 Nov 7	1920	0.52	21.14	20.52	9.3×10^{-18}	3.2	3
				$H_2(2-1)$	2003 Nov 7	5760	0.52	20.74	20.07			

[a] The 3 σ detection limit of the Hα emission line.

[b] The 3 σ detection limit of the SFR.

[c] Observed with UKIRT + UFTI.

[d] Observed with Subaru + CISCO.

REFERENCES.—(1) Crotts & Fang 1998; (2) Steidel 1990, Cowie et al. 1995, Dobrzycki & Bechtold 1991; (3) Teplitz et al. 1998.

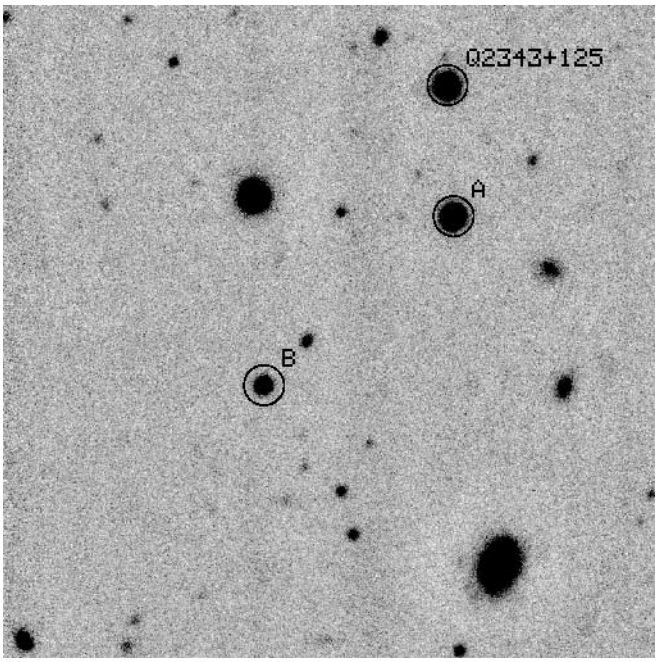

FIG. 1.—The K' image of the field around Q2343+125. The quasar and two objects that have color excesses in NB filters are surrounded by circles. The FOV of the images is $94''.5 \times 94''.5$ (slightly trimmed from the observed image), which corresponds to 512 h^{-1} kpc $\times$ 512 h^{-1} kpc at $z \sim 2.43$.

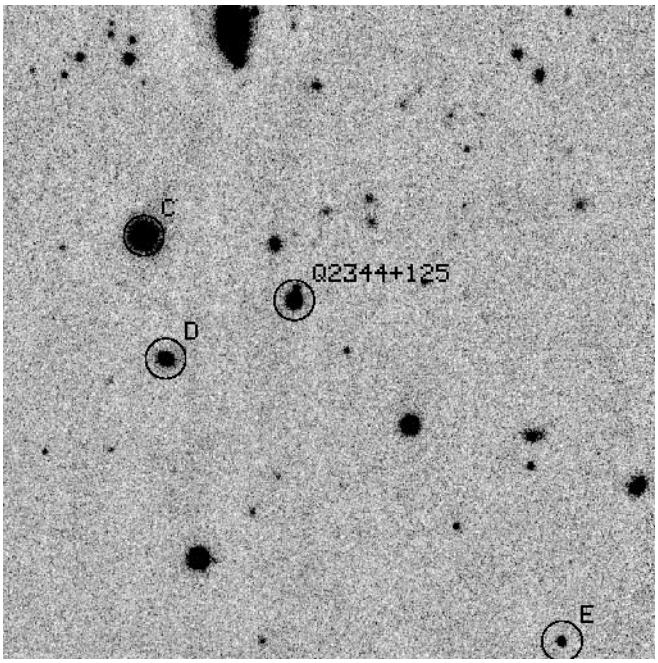

FIG. 2.—Same as Fig. 1, but for the field around Q2344+125.

From the luminosity of the Hα emission line, $L_{H\alpha}$ (ergs per second), we can also evaluate the star formation rate (SFR) using the conversion relation described in Kennicutt (1998),

$$\mathrm{SFR}_{H\alpha}(\mathrm{total}) = \frac{L_{H\alpha}}{1.27 \times 10^{41}\ \mathrm{ergs\ s^{-1}}}\ M_\odot\ \mathrm{yr}^{-1}, \qquad (3)$$

where we assume the Salpeter initial mass function with lower and upper mass cutoffs of 0.1 and 100 $M_\odot$, respectively.

4. RESULTS

The CM analysis of all the objects detected in the six fields around pair/triple quasars yielded two and three candidates for star-forming galaxies around Q2343+125 and Q2344+125, respectively. In this section, we describe the result for each quasar field.

4.1. *KP 76/KP 77/KP 78*

The quasar triplet (KP 76: Q1623+2651A at $z_{em} = 2.467$, KP 77: Q1623+2653 at $z_{em} = 2.526$, and KP 78: Q1623+2651B at $z_{em} = 2.605$) is located on the sky within a small FOV of 3′: 147″ between KP 76 and KP 77, 127″ between KP 76 and KP 78, and 177″ between KP 77 and KP 78 (e.g., Crotts & Fang 1998). All of them have C IV absorption lines at $z \sim 2.24$ in their spectra with total equivalent widths, $W_{rest} \sim 0.14$, 0.08, and 2.34 Å, respectively. Other transitions of metal lines, such as C I, C II, Si II, Si III, Si IV, and N V, are also identified. The radial velocity separations of these absorption lines are within 500 km s^{-1} of each other in the frame of the absorbers. The linear angular distance on the sky between these systems corresponds to $\sim 1\ h^{-1}$ Mpc at $z \sim 2.24$, which is comparable to the typical size of a cluster of galaxies in the local universe.

We carried out two deep imaging observations of the fields around KP 76 with UKIRT + UFTI with FOV of 90″ × 90″ (i.e., 500 h^{-1} kpc × 500 h^{-1} kpc) and KP 77/KP 78 with Subaru + CISCO with FOV of 108″ × 108″ (i.e., 600 h^{-1} kpc × 600 h^{-1} kpc). Although we found two objects around KP 76 that were detected only in NB filters, they are confirmed to be ghost images of the brightest sources in the frames. There are not any other candidates for star-forming galaxies with SFR $> 6.8\ h^{-2}\ M_\odot\ \mathrm{yr}^{-1}$ ($f_{H\alpha} > 2.4 \times 10^{-17}$ ergs s^{-1} cm^{-2}) in the KP 76 field or SFR $> 1.8\ h^{-2}\ M_\odot\ \mathrm{yr}^{-1}$ ($f_{H\alpha} > 6.3 \times 10^{-18}$ ergs s^{-1} cm^{-2}) in the KP 77/KP 78 field, with a 3 σ detection limit of $K' \leq 21$.

4.2. *Q0301−005/Q0302−003*

This pair quasar is separated by about 17′ from each other on the sky, which corresponds to $\sim 5.5\ h^{-1}$ Mpc at $z \sim 2.43$ (e.g., Dobrzycki & Bechtold 1991). They have common C IV and/or Si IV doublets at $z \sim 2.96$, 2.72, and 2.43 (Cowie et al. 1995; Songaila 1998; Steidel 1990), of which only Hα emission at $z \sim 2.43$ can be identified by the NB filter of our observation. We took two images with UKIRT + UFTI around both quasars by putting them at the centers of frames. We identified no candidates for star-forming galaxies with SFR $> 236\ h^{-2}\ M_\odot\ \mathrm{yr}^{-1}$ ($f_{H\alpha} > 6.9 \times 10^{-16}$ ergs s^{-1} cm^{-2}) in the Q0301 field and SFR $> 23\ h^{-2}\ M_\odot\ \mathrm{yr}^{-1}$ ($f_{H\alpha} > 6.7 \times 10^{-17}$ ergs s^{-1} cm^{-2}) in the Q0302 field. The 3 σ detection limits are $K' = 20.1$ around Q0301−005 and $K' = 21.1$ around Q0302−003.

4.3. *Q2343+125/Q2344+125*

Q2343+125 has C IV absorption lines at $z = 2.4285$ and 2.4308, while Q2344+125 has corresponding strong C IV absorption lines at $z = 2.4265$ and 2.4292 (Sargent et al. 1988). The velocity separation of these absorption lines along the line of sight is smaller than 400 km s^{-1}. These quasars are separated from each other only by 5′ ($\sim 1.6\ h^{-1}$ Mpc) at $z \sim 2.43$. The C IV absorption system in Q2343+125, which was classified as a damped Lyα system (Lu et al. 1998), has other metal lines such as Al II λ1670, Fe II λ1608, and Si II λ1526.

To date, several deep imaging observations have been carried out for this field. Bergvall et al. (1997) took optical NB deep images to search for Lyα-emitting objects around both of the quasars but did not find any candidates. Lyα emission, however, is strongly affected by dust extinction, which makes it difficult to

TABLE 3
CANDIDATES FOR Hα EMITTERS

Field (1)	Object (2)	K' (mag) (3)	$f_{\mathrm{H}\alpha}$[a] (ergs s^{-1} cm^{-2}) (4)	SFR ($h^{-2}\ M_\odot$ yr^{-1}) (5)	FWHM (arcsec) (6)
Q2343+125	A	14.92	1.35×10^{-15}	466	0.97
	B	16.87	2.17×10^{-16}	75	0.99
Q2344+125	C	16.29	3.14×10^{-16}	108	0.82
	D	17.64	9.34×10^{-17}	32	0.80
	E	18.28	5.67×10^{-17}	20	0.65

[a] Total flux of Hα emission line, without a correction for the effects of the [N II] line.

detect. Therefore, Teplitz et al. (1998) took deep NIR images with a small FOV ($38'' \times 38''$) around Q2343+125 to search for Hα emitters, but nothing was detected. Bunker et al. (1999) also carried out a long-slit K-band spectroscopic search for Hα emitters in the vicinity (within $11'' \times 2\farcs5$) of Q2343+125 but found nothing above the 3 σ limit [$f_{\mathrm{H}\alpha} = (6.5\text{–}16) \times 10^{-17}$ ergs s^{-1} cm^{-2}].

In our NIR images taken with Subaru + CISCO, we detected two candidates (objects A and B) for star-forming galaxies at $z \sim 2.43$ around Q2343+125 (Fig. 1) and three candidates (objects C, D, and E) around Q2344+125 (Fig. 2), whose K' magnitude, Hα flux, and SFR are listed in Table 3, by assuming that they are actually galaxies at $z \sim 2.43$. Unfortunately, it is difficult to tell the morphological type of the identified objects because of low spatial resolution in the observed images. The 3 σ detection limits of these images are $K' = 20.5$ and 21.1, respectively. These objects were outside of the frame (or just at the borders of the FOV) in the previous observation by Teplitz et al. (1998). The CM diagrams are also presented in Figures 3 and 4. All candidates are bright ($K' < 18.3$) and their apparent SFRs are very large (>20 $h^{-2}\ M_\odot$ yr^{-1}). We discuss them in § 5.

5. SUMMARY AND DISCUSSION

We detected five candidates (objects A–E) for intervening galaxies around two of six pair/triple quasar fields by NIR NB imaging observations. They are all bright ($K' < 18.3$) with large Hα fluxes ($f_{\mathrm{H}\alpha} > 5.7 \times 10^{-17}$ ergs s^{-1} cm^{-2}).

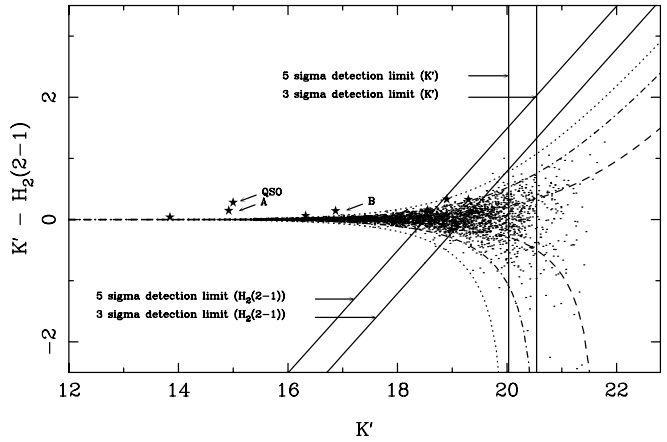

FIG. 3.—The K' − NB [H_2(2–1)] color vs. K' diagram for the field around Q2343+125. The stars denote the objects detected in both K' and NB images, while the dots represent the simulated data (only 1 of every 10 data points is plotted to make them easy to see). The three marked objects are a quasar and candidates for Hα-emitting galaxies at $z \sim 2.43$. Dashed, dot-dashed, and dotted curves are 1, 2, and 3 σ deviations of the artificial objects placed in the CM diagram, respectively. Solid lines denote 3 and 5 σ detection limits in K' and NB frames.

Teplitz et al. (1998) detected 13 Hα emitters, using the same method as ours, of which the brightest two objects ($K' = 15.42$ with $f_{\mathrm{H}\alpha} = 249 \times 10^{-17}$ ergs s^{-1} cm^{-2} around Q0114−089 and $K' = 18.15$ with $f_{\mathrm{H}\alpha} = 581 \times 10^{-17}$ ergs s^{-1} cm^{-2} around PC 2149+0221) have similar properties to ours. Teplitz et al. (1998) regarded them as Seyfert I galaxies, because they are extremely compact and one of them has broad emission lines. However, all (or at least a substantial fraction) of our objects with absolute magnitude $M_B < -24 + 5 \log h$ are not likely to be Seyfert galaxies at $z \sim 2.43$, because their volume density[8] (∼5.2 h^3 Mpc^{-3}) is much larger than the global density of active galactic nuclei with similar luminosities at similar redshifts (∼10^{-6} Mpc^{-3}; Warren et al. 1994). Some of them could be foreground (active) galaxies at $z \sim 0.04$, 0.20, 0.37, 0.76, and 0.79, whose Brγ, Paα, [Fe II] 1.644 μm, Paβ, and [Fe II] 1.257 μm emission lines, respectively, are redshifted into the bandpass of NB filters. These are the most prominent emission lines of active galaxies in the NIR window (e.g., Simpson et al. 1996; Kawara et al. 1988; Goodrich et al. 1994). Actually, Tamura et al. (2001) found a galaxy at $z = 0.132$ whose Paα is strong, $f_{\mathrm{Pa}\alpha} = 3.4 \times 10^{-17}$ ergs s^{-1} cm^{-2} with NB imaging observation. Thus, it seems unlikely that there exists a cluster (group) of bright galaxies at $z \sim 2.43$.

In the fields of other pair/triple quasars, we detected no galaxies at redshifts of the common C IV absorption lines. There are at least four possible reasons.

[8] We evaluated this value by assuming that all five objects exist within 1.6 h^{-1} Mpc from each other along the line of sight, which is consistent with the separation of the lines of sight to the pair quasars at $z \sim 2.43$.

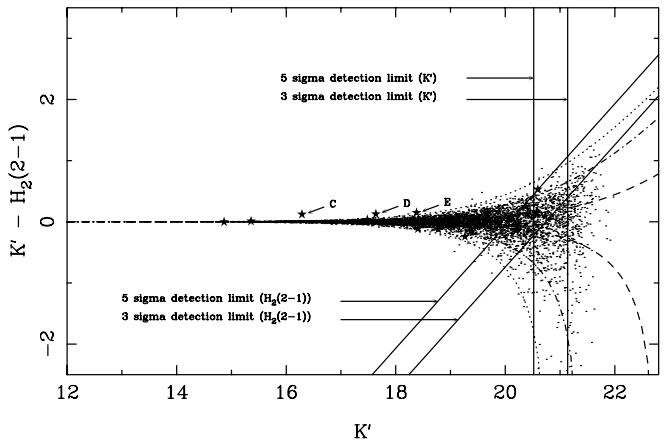

FIG. 4.—Same as Fig. 3, but for the field around Q2344+125. The quasar is not plotted, because we do not plot objects that are blended with their neighbors, as the quasar is.

First, this could be because the SFRs are too low to detect in the observed frames. The minimum SFR and Hα flux we can detect in each observed frame is described in § 4 and summarized in Table 2. Typical SFRs of individual field galaxies at $z \sim 2$ have been estimated to be $\sim$10–35 $M_\odot$ yr^{-1} (without a dust extinction correction) by IR imaging surveys with NB filters and spectroscopic observations (e.g., Moorwood et al. 2000; Iwamuro et al. 2000). Similar SFRs are derived for Lyman break galaxies at $z \sim 2$–3 from spectroscopic observations of Hβ emission lines ($\sim$20–70 $M_\odot$ yr^{-1}, with one exception of $\sim$270 $M_\odot$ yr^{-1}; Pettini et al. [1998]). Juneau et al. (2005) also estimated SFRs of field galaxies at $z \sim 2$ from ultraviolet continuum luminosities corrected for dust extinction and got similar values ($\sim$30 $M_\odot$ yr^{-1}). Teplitz et al. (1998) searched star-forming galaxies at the same redshift as the metal absorption systems and found 11 Hα emitters at $z = 2.3$–2.5 within 250 kpc of quasar lines of sight. Their average SFR is $\sim$50 $M_\odot$ yr^{-1}. The 3 σ detection limits of the SFR in the Q0301/Q0302 fields are comparable to or larger than the average SFR at $z \sim 2$ in the literature. In this case, star-forming galaxies could not be detected unless they have extremely large SFRs. On the other hand, the image depths of the other fields are enough to detect field star-forming galaxies with typical SFRs, which means that absorbers corresponding to C IV absorption lines could have lower SFRs, compared with field galaxies at the same redshift.

The second possible reason for nondetection is that typical star-forming galaxies could be faint compared to the detection limits of our observations. At $z \sim 2$, the average K' magnitude of star-forming galaxies detected based on metal absorption lines is $K' \sim 20.8$ (Teplitz et al. 1998). On the other hand, of six fields observed, one (or four) fields were observed to provide images deep enough to detect such faint star-forming galaxies with a 5 σ (or 3 σ) detectability. Although the observed images are very deep for most fields, they were not deep enough for some fields (i.e., the Q0301 and Q2343 fields). We also confirmed that there is no number excess of galaxy counts in the fields around the pair quasars (Fig. 5), compared with the global value of field galaxies around the Subaru Deep Field (Maihara et al. 2001). Thus, we cannot yet reject the existence of clusters (groups) of galaxies in our pair/triple quasar fields, because they could contain only faint galaxies with $K' \geq 21$.

Third, it is also possible that our targeting fields did not cover star-forming galaxies by chance. We calculated field coverage fractions (i.e., ratio of the area covered by our observations to the area of the pair quasar field).[9] We got large values of $\sim$75% and 33% for the KP 76/KP 77/KP 78 and Q2343/Q2344 fields, respectively, while the coverage fraction for the Q0301/Q0302 field is very small, $\sim$2%. It seems unlikely that we happened to miss both star-forming galaxies and a number excess of galaxies in the fields around KP 76/KP 77/KP 78 and Q2343/Q2344 pair/triple quasars, if clusters of galaxies really exist there. In the case of the Q0301/Q0302 field, the result is still open to some uncertainties (e.g., the coverage fraction could be underestimated, if galaxies are distributed not spherically but filamentarily on the scale of $\sim$5 Mpc along the pair quasars).

Finally, most C IV lines, whose counterparts were not identified, could arise in star-forming pockets outside bright galaxies (e.g., the ejecta of Type Ia supernovae, dwarf galaxies, or low surface brightness galaxies), which have already been suggested as counterparts of weak ($W_{\rm rest} < 0.3$ Å) Mg II lines (Rigby et al. 2002). These pockets have multiple phases: a kiloparsec-scale, higher ionization phase that produces C IV and a compact-scale ($\sim$10 pc), low-ionization phase with high density that produces Mg II (Charlton et al. 2003). The redshift path density of weak Mg II systems is twice that of the strong Mg II systems, which have almost always corresponding luminous galaxies (Steidel 1995). Weak Mg II systems also have high (solar or supersolar) metallicities (Charlton et al. 2003). Nevertheless, corresponding luminous galaxies are rarely found within $\sim$50 h^{-1} kpc of the quasars (Churchill et al. 1999). All the properties of weak Mg II systems are consistent with the nondetection of star-forming galaxies in our observations.

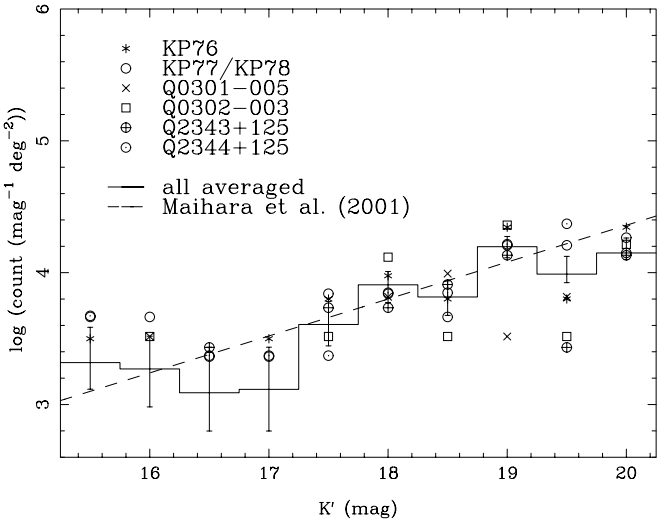

FIG. 5.—Galaxy number count (mag^{-1} deg^{-2}) vs. K' magnitude in each pair quasar field. We do not plot marks if no objects were found in a given bin of K' magnitude in some quasar fields. The histogram with 1 σ errors denotes the number counts averaged in all six fields. We also overlaid the number count of field galaxies evaluated in the Subaru Deep Field (Maihara et al. 2001). We adopted *best* magnitudes (see SExtractor program manual; Bertin & Arnouts [1996]) in this plot to compare them directly with Maihara et al.'s result.

With K-band imaging observations, we placed photometric and SFR upper limits of Hα emitters corresponding to C IV absorption lines toward the lines of sight of pair/triple quasars. Deeper imaging surveys for wider fields that completely cover pair/triple quasar fields are necessary before concluding whether galaxy clusterings corresponding to metal absorption lines really exist or not. A large number of multiple quasars have also recently been discovered by large-scale surveys such as the Sloan Digital Sky Survey (Schneider et al. 2005) and the 2dF QSO Redshift Survey (Croom et al. 2004), which will enable us to extend this survey in the future.

Part of our observations were kindly carried out during the engineering time of the Subaru Telescope. We would like to thank J. C. Charlton and M. Eracleous for their comments that helped in developing this study and I. Tanaka and M. Kajisawa for their useful advice on reduction of infrared data. We also would like to thank D. Tytler and V. D'Odorico for informing us of the coordinates of one of our targets. Finally, we wish to thank the anonymous referee for many helpful comments and suggestions.

[9] This area is the area of the circles on which all pair/triple quasars are located. For example, this area would be evaluated to be $\pi(150'')^2$ for the Q2343/Q2344 pair quasars that are separated by 300″ from each other on the sky. Areas used here are the lower limit of the size of a possible cluster (group) of galaxies, because member galaxies are probably distributed outside of these circles if such galaxies really exist.

REFERENCES

Bergeron, J., & Boissé, P. 1991, A&A, 243, 344
Bergvall, N., Östlin, G., Karlsson, K. G., Örndahl, E., & Rönnback, J. 1997, A&A, 321, 771
Bertin, E., & Arnouts, S. 1996, A&AS, 117, 393
Bunker, A. J., Warren, S. J., Clements, D. L., Williger, G. M., & Hewett, P. C. 1999, MNRAS, 309, 875
Charlton, J. C., & Churchill, C. W. 1996, ApJ, 465, 631
Charlton, J. C., Ding, J., Zonak, S. G., Churchill, C. W., Bond, N. A., & Rigby, J. R. 2003, ApJ, 589, 111
Chen, H.-W., Lanzetta, K. M., & Webb, J. K. 2001a, ApJ, 556, 158
Chen, H.-W., Lanzetta, K. M., Webb, J. K., & Barcons, X. 2001b, ApJ, 559, 654
Churchill, C. W., Rigby, J. R., Charlton, J. C., & Vogt, S. S. 1999, ApJS, 120, 51
Cowie, L. L., Songaila, A., Kim, T.-S., & Hu, E. M. 1995, AJ, 109, 1522
Croom, S. M., Smith, R. J., Boyle, B. J., Shanks, T., Miller, L., Outram, P. J., & Loaring, N. S. 2004, MNRAS, 349, 1397
Crotts, A. P. S., & Fang, Y. 1998, ApJ, 502, 16
Dobrzycki, A., & Bechtold, J. 1991, ApJ, 377, L69
Francis, P. J., & Hewett, P. C. 1993, AJ, 105, 1633
Francis, P. J., Woodgate, B., & Danks, A. C. 1997, ApJ, 482, L25
Francis, P. J., et al. 1996, ApJ, 457, 490
Goodrich, R. W., Veilleux, S., & Hill, G. J. 1994, ApJ, 422, 521
Hu, E. M., & McMahon, R. G. 1996, Nature, 382, 231
Iwamuro, F., et al. 2000, PASJ, 52, 73
Iye, M., et al. 2004, PASJ, 56, 381
Jakobsen, P., Perryman, M. A. C., Ulrich, M. H., Macchetto, F., & di Serego Alighieri, S. 1986, ApJ, 303, L27
Juneau, S., et al. 2005, ApJ, 619, L135
Kawara, K., Nishida, M., & Taniguchi, Y. 1988, ApJ, 328, L41
Kennicutt, R. C., Jr. 1998, ARA&A, 36, 189
Lanzetta, K. M., Chen, H.-W., Webb, J. K., & Barcons, X. 1998, in IAU Colloq. 171, The Low Surface Brightness Universe, ed. J. I. Davies, C. Impey, & S. Phillipps (ASP Conf. Ser. 170; San Francisco: ASP), 35
LeFèvre, O. L., Deltorn, J. M., Crampton, D., & Dickinson, M. 1996, ApJ, 471, L11
Lu, L., Sargent, W. L. W., & Barlow, T. A. 1998, AJ, 115, 55
Maihara, T., et al. 2001, PASJ, 53, 25
Moorwood, A. F. M., van der Werf, P. P., Cuby, J. G., & Oliva, E. 2000, A&A, 362, 9
Motohara, K., et al. 1998, Proc. SPIE, 3354, 659
Pascarelle, S. M., Windhorst, R. A., Driver, S. P., Ostrander, E. J., & Keel, W. C. 1996, ApJ, 456, L21
Pentricci, L., et al. 2000, A&A, 361, L25
Pettini, M., Kellogg, M., Steidel, C. C., Dickinson, M., Adelberger, K. L., & Giavalisco, M. 1998, ApJ, 508, 539
Rigby, J. R., Charlton, J. C., & Churchill, C. 2002, ApJ, 565, 743
Roche, P. F., et al. 2003, Proc. SPIE, 4841, 901
Sargent, W. L. W., Boksenberg, A., & Steidel, S. S. 1988, ApJS, 68, 539
Schneider, D. P., et al. 2005, AJ, 130, 367
Shaver, P. A., Boksenberg, A., & Robertson, J. G. 1982, ApJ, 261, L7
Simpson, C., Forbes, D. A., Baker, A. C., & Ward, M. J. 1996, MNRAS, 283, 777
Songaila, A. 1998, AJ, 115, 2184
Steidel, C. C. 1990, ApJS, 74, 37
———. 1995, in QSO Absorption Lines, ed. G. Meylan (Berlin: Springer), 139
Steidel, C. C., Dickinson, M., & Persson, S. E. 1994, ApJ, 437, L75
Tamura, N., Ohta, K., Maihara, T., Iwamuro, F., Motohara, K., Takata, T., & Iye, M. 2001, PASJ, 53, 653
Teplitz, H. I., Malkan, M., & McLean, I. S. 1998, ApJ, 506, 519
Warren, S. J., Hewett, P. C., & Osmer, P. S. 1994, ApJ, 421, 412